JACS
JOURNAL OF THE AMERICAN CHEMICAL SOCIETY

ARTICLE

pubs.acs.org/JACS

Nanoparticle Shape Anisotropy Dictates the Collective Behavior of Surface-Bound Ligands

Matthew R. Jones,[†,§] Robert J. Macfarlane,[‡,§] Andrew E. Prigodich,[‡,§] Pinal C. Patel,[‡,§] and Chad A. Mirkin*[,†,‡,§]

[†]Department of Materials Science and Engineering, [‡]Department of Chemistry, and [§]International Institute for Nanotechnology, Northwestern University, 2145 Sheridan Road, Evanston, Illinois 60208-3113, United States

Supporting Information

ABSTRACT: We report on the modification of the properties of surface-confined ligands in nanoparticle systems through the introduction of shape anisotropy. Specifically, triangular gold nanoprisms, densely functionalized with oligonucleotide ligands, hybridize to complementary particles with an affinity that is several million times higher than that of spherical nanoparticle conjugates functionalized with the same amount of DNA. In addition, they exhibit association rates that are 2 orders of magnitude greater than those of their spherical counterparts. This phenomenon stems from the ability of the flat, extended facets of nonspherical nanoparticles to (1) support more numerous ligand interactions through greater surface contact with complementary particles, (2) increase the effective local concentration of terminal DNA nucleotides that mediate hybridization, and (3) relieve the conformational stresses imposed on nanoparticle-bound ligands participating in interactions between curved surfaces. Finally, these same trends are observed for the pH-mediated association of nanoparticles functionalized with carboxylate ligands, demonstrating the generality of these findings.

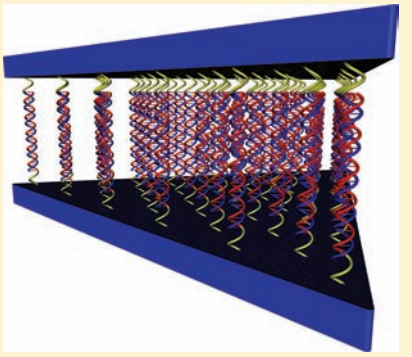

INTRODUCTION

It is well established that the size of a nano-object significantly affects its physical properties. However, recent interest has centered around the concept of nanoparticle shape and the properties that arise from geometric anisotropy.[1,2] Particularly for the noble metal nanostructures, shape has been shown to give rise to a number of effects, including wavelength-tunable surface plasmon resonances,[3,4] electromagnetic field concentration,[5] and surface-facet-selective catalytic activity,[6] to name a few. Interestingly, while many of these physical properties have been thoroughly investigated, relatively few studies have investigated how shape affects the collective behavior of surface-bound ligands.[7,8] Although a variety of molecules have been successfully conjugated to nanoparticle surfaces, DNA ligands provide an ideal platform for probing the influence of particle shape because both their thermal properties (hybridization and melting behavior) and their structural properties (conformation and helical pitch) are well understood. In addition, DNA-functionalized gold nanoparticles (DNA-AuNPs) have been shown to exhibit unique properties that can be directly linked to a dense surface coverage of oligonucleotides.[9−12] These include sharp melting transitions when hybridized to complementary particles (where "melting" refers to the dehybridization of DNA-AuNPs),[9] elevated binding constants for the capture of free DNA,[10] and the ability to naturally transfect cells.[11] Because these properties originate from the polyvalent nature of the anchored oligonucleotides, one can hypothesize that changing the shape of the underlying Au nanoparticle scaffold will result in dramatic modifications to the hybridization behavior of DNA-AuNPs. Here we show that DNA-functionalized anisotropic nanoparticles are capable of both thermodynamic and kinetic enhancement to interparticle hybridization compared to their isotropic (spherical) counterparts (Figure 1a). Additionally, carboxylate-terminated ligands are shown to exhibit the same qualitative behavior, suggesting the effects elucidated here are applicable to range of nanoparticle−ligand combinations. Importantly, these properties depend solely on the presence of anisotropy in the interactions between the surrounding ligand shells and give some of the first indications that nonspherical nanoparticle scaffolds can modulate the behavior of molecules conjugated to their surfaces.

While the role of nanoparticle size in interparticle association has been explored by a variety of researchers,[13−16] few have investigated the role of anisotropy. Nonspherical nanostructures provide advantages in understanding the collective properties of ligand shells in two primary ways. First, the majority of synthetic methods for colloidal anisotropic nanoparticles produce structures that consist entirely of flat surfaces in the form of crystallographic facets.[1] Use of these particles allows one to fully account for and understand radius of curvature effects, which have been shown to affect hybridization in DNA-AuNP systems.[16,17] Second, nanoparticle anisotropy imparts a form of

Received: July 20, 2011
Published: November 01, 2011

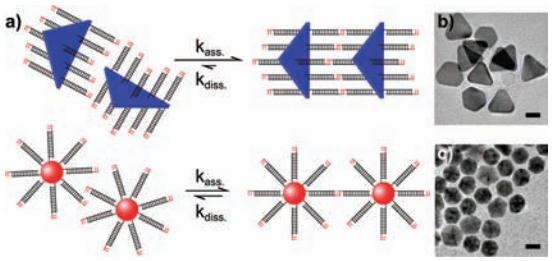

Figure 1. (a) Simplified scheme of the preferential association between anisotropic triangular nanoprisms compared to spherical nanoparticles, as a result of shape-mediated modifications to their surface ligand shells. Triangular prism particles facilitate a higher rate of particle association ($k_{ass.}$) and a lower rate of particle dissociation ($k_{diss.}$) than their spherical counterparts. DNA base-pairing of the red terminal nucleotides provides the driving force for association. (b,c) TEM images of the nanoprisms (b) and spheres (c) used in this work (scale bars are 20 nm).

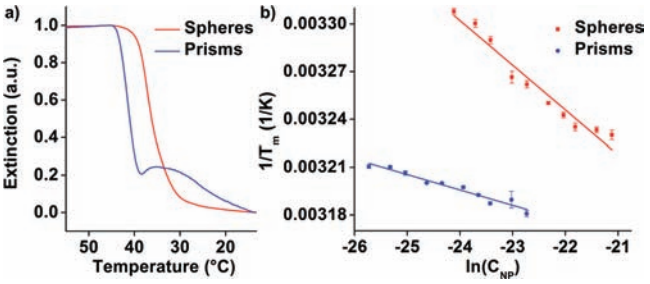

Figure 2. (a) Analysis of nanoparticle hybridization by monitoring SPR as a function of temperature. From high (left side of graph) to low (right side of graph) temperatures, nanoparticles undergo a rapid, DNA-mediated change from a discrete state to one where particles are completely bound, described by a characteristic transition temperature T_m. (b) Linear interpolation of concentration-dependent transition temperatures allows for quantification of the equilibrium constant for nanoparticle hybridization from fundamental thermodynamic parameters. This analysis reveals the equilibrium constant for interparticle prism hybridization to be 6 orders of magnitude greater than that for spheres.

valency in the interactions between particles, where particular interparticle orientations or directions of interaction are more favorable than others. Indeed, calculation of the fraction of ligands bound in a two-particle association process show that more bonds are made as the constituent nanoparticles become more anisotropic (Supporting Information, Figure S1). This suggests that new properties might arise in nanoparticle interactions that are unique to structures with obvious anisotropy. To probe the effects of nanoparticle shape on the interparticle hybridization process, gold triangular nanoprisms were chosen as a model system to compare to spherical particles. Triangular nanoprisms (henceforth referred to as "prisms" for convenience) are a unique nanostructure in that they consist primarily of two extended, atomically flat {111} faces and are significantly wider than they are thick.[18] As a result, they are essentially two-dimensional nanoscale objects and are among the most anisotropic shapes that are synthetically available (Figure S2). Furthermore, prisms and spheres show the greatest disparity in initial calculations detailing the percentage of ligands bound in a simple oriented association model (Figure S1). This suggests that any differences in the behavior of the ligand shells as a function of nanoparticle shape will be most pronounced for this pair of structures. DNA-Au nanoprisms therefore provide an ideal platform for investigating shape-mediated ligand effects by using the context of DNA-directed interparticle hybridization as a probe for ligand activity.

RESULTS AND DISCUSSION

Gold triangular nanoprisms and spherical gold nanoparticles were synthesized and functionalized with oligonucleotides containing a terminal alkylthiol moiety according to literature precedent (see Supporting Information for details).[19,20] Next, complementary linker oligonucleotides were added to induce interparticle association. These linkers consist of a recognition sequence that binds to the strands anchored on the particle surface and present a short, terminal, self-complementary "sticky end" ($^{5'}$TGCA$^{3'}$) which facilitates hybridization between DNA-AuNPs (Figure 1a). This design lets the majority of the bases in a given strand be duplexed and rigid, allowing the ligands to preserve the shape of the nanoparticle to which they are attached, while also localizing the short, sticky-end bases that link particles together to a small volume around the periphery of the particle. DNA loading assays were conducted on a range of prism and sphere sizes in order to compare particles with equivalent numbers of oligonucleotides (Figure S3). By selecting particle sizes such that each shape has the same number of oligonucleotides, one can ensure that prisms and spheres have the same opportunity for binding and that any differences observed are due to anisotropy effects. It was determined that prisms with an edge length of ~40 nm (thickness of ~7 nm) and spheres with a diameter of ~22 nm have the same average number of strands per particle (~270 DNA molecules), and therefore were compared in all subsequent hybridization experiments (Figure 1b,c).

To investigate the thermodynamics of DNA-mediated AuNP association, equilibrium constants were derived from concentration-dependent hybridization studies. Specifically, solutions containing prisms, spheres, and linker oligonucleotides were slowly cooled from 60 to 10 °C. By monitoring the surface plasmon resonance (SPR) of the spherical particles (530 nm) and the nanoprisms (750 nm) as a function of temperature, the hybridization transition (T_m) of each species could be determined, as interparticle association results in large shifts in the SPR peak position and intensity (Figure 2a).[21] At high temperatures, both the nanoprisms and spherical particles are discrete and dispersed. As the temperature is decreased, a sharp drop in the extinction is observed, indicating oligonucleotide-mediated aggregation. The higher temperature at which the prisms hybridize demonstrates that they are able to stabilize interparticle interactions more readily than spheres. This effect can be quantified by repeating the experiment at different nanoparticle concentrations (C_{NP}) and plotting $1/T_m$ against values of $\ln(C_{NP})$ according to the following equation (Figure 2b):

$$\frac{1}{T_m} = \frac{R}{\Delta H^\circ} \ln C_{NP} + \frac{\Delta S^\circ}{\Delta H^\circ}$$

The linear relationship allows for determination of the enthalpy (ΔH°) and entropy (ΔS°) of association, from which the equilibrium constant can be calculated following literature methods (see Supporting Information).[10,22,23] The results of this analysis reveal a dramatic thermodynamic preference for prism association over sphere association by a factor of over 10^6 (spheres and prisms have binding constants of 1.5×10^{11} and 5.3×10^{17} M^{-1}, respectively). Note that these equilibrium constants are relevant for the case where the initial state is

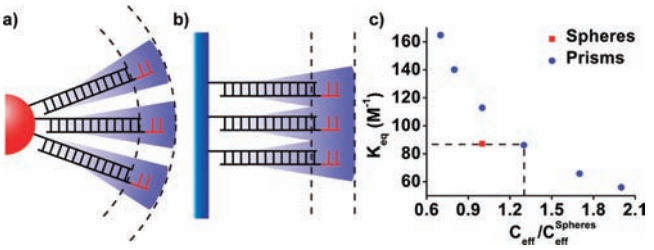

Figure 3. Schematic illustration of the effective concentration of DNA "sticky ends" surrounding spheres (a) and prisms (b). Although the surface density of ligands on spheres is higher, the prism shape more effectively concentrates the terminal nucleotides, thus increasing the "on" rate for DNA hybridization and decreasing $k_{diss.}$. (c) Quantification of the prism effective concentration by comparison of the sticky-end binding constants on spheres (red) and prisms (blue). A factor of 1.3 elevation in the effective concentration of DNA sticky ends surrounding prisms is necessary for each system to exhibit the same K_{eq}.

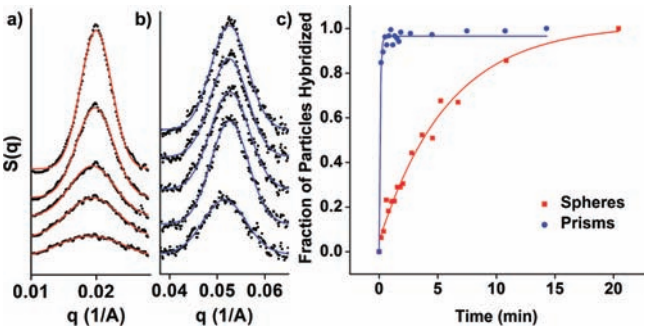

Figure 4. SAXS diffraction peaks for associating spheres (a) and prisms (b) at roughly equivalent time points. Curves are offset for clarity, with reaction time increasing from bottom to top (0.25, 0.65, 1.5, 4.5, 10.8 min). A more rapid increase in intensity and narrowing of the prism peaks indicate faster interparticle association. (c) Quantification of the growth of nanoparticle aggregates over time, showing a ~60-fold faster association for prisms over spheres.

described by a solution of discrete, minimally interacting particles, and the final state is described by a completely hybridized aggregate of particles.

We propose that the origin of the enhanced binding strength for anisotropic nanostructures arises directly from the particle shape in three primary ways. First, previous results indicated that nanoprisms associate in a face-to-face manner, while spheres associate isotropically.[8,15] This allows for the extended 2D faces of the nanoprisms to facilitate a greater number of oligonucleotide duplexes than similarly functionalized spherical particles. This property has the effect of deflating the rate of particle dissociation ($k_{diss.}$), as more connections must be broken to release hybridized prisms than hybridized spheres.

A second effect induced by nanoparticle shape is the preorganization of oligonucleotides off the surface of the prisms in an arrangement that is optimized for maximum interparticle binding. This can be equivalently represented as a higher "effective" concentration (C_{eff}) of oligonucleotide sticky ends surrounding the prism surface, which serves to elevate the "on" rate for individual DNA duplex formation, thereby elevating the $k_{ass.}$ for the nanoparticles (Figure 3a,b). Furthermore, DNA duplexes that dehybridize are able to immediately rehybridize, resulting in a depression of $k_{diss.}$.[15] Since an individual DNA sticky end should exhibit the same thermodynamic behavior regardless of the nanoparticle substrate to which it is anchored, one can estimate the effective concentration of DNA sticky ends by comparing their binding constants on spheres and prisms (Figure 3c). In this analysis, the effective sticky-end concentration surrounding spheres is estimated according to literature precedent (red point, Figure 3c),[15] and the prism effective sticky-end concentration is calculated using multiples of this value (blue points, Figure 3c). In order for the sticky-end sequences to exhibit identical thermodynamic behavior, their individual binding constants on prisms and spheres must be the same. This occurs when the prism effective sticky-end concentration is 1.3 times that of the spheres, indicating a 30% greater efficiency with which prisms can concentrate terminal nucleotide bases. Importantly, this effect most strongly influences the behavior of discrete DNA strands by modifying their local chemical environment, while the previous effect is more active at the nanoparticle level, where the collective behavior of many oligonucleotide ligands dictates the performance of the system.

A third mechanism is that prism−prism association allows individual DNA duplexes to be more stable than those linking spheres, as the geometry of the interaction minimizes the need for strands to adopt unfavorable conformations. This model is corroborated by measurements of the rise per base-pair for spherical (0.255 nm/bp)[15] and nanoprism (0.281 nm/bp)[8] aggregates, which suggests a more strained conformation for the DNA that is linking spherical particles than that linking prisms (typically DNA exhibits a value of 0.29−0.34 nm/bp).[23] Because spherical particles are highly curved, oligonucleotides will be required to bend or compress to form complementary duplexes with neighboring particles, thus decreasing their thermodynamic stability.[15] Other effects, such as localization of salt between flat prism surfaces, may contribute to the observed enhancement but are challenging to probe experimentally and will be the subject of further investigations.

Since these results indicate a thermodynamic binding dependence on DNA-AuNP shape, one can postulate that the kinetics of association may also be altered by nanoparticle anisotropy. To test this hypothesis, time-resolved small-angle X-ray scattering (SAXS) was used to monitor the formation rate of nanoparticle aggregates. Separate solutions of prisms and spheres with equal nanoparticle concentration (200 pM) were combined with excess linker oligonucleotides and rapidly cooled from 60 to 20 °C, where both species can form stable interparticle linkages. By tracking the full width at half-maximum of the scattering peaks as a function of time (Figure 4a,b), the fraction of hybridized nanoparticles could be determined from the growth of the aggregate domain size (see Supporting Information for full analysis).[24] Under these conditions, the prism association is complete in seconds, while the spherical particles require several minutes to fully hybridize and aggregate (Figure 4c). Quantification of the half-life for each reaction reveals the observed rate for prism hybridization to be approximately 2 orders of magnitude faster than sphere hybridization (spheres and prisms have $t_{1/2}$ values of 3.68 and 0.0614 min, respectively).

The kinetic enhancement can be understood by the same mechanisms that govern the thermodynamic enhancement. With a greater number of interparticle linkages due to the commensurate and parallel orientation of the nanoprism faces, the rate of particle dehybridization is significantly depressed, as numerous connections must be severed simultaneously to release bound

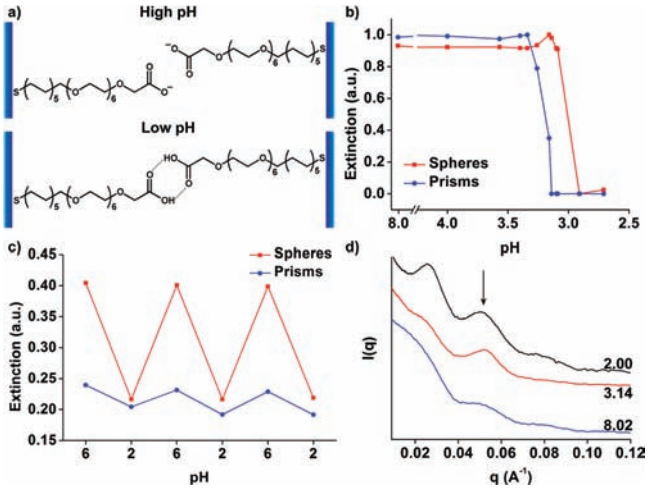

Figure 5. (a) Illustration of the hydrogen-bonding interactions between terminal carboxylic acid groups, as a function of solution pH, that mediate interparticle association. (b) Monitoring the SPR of each nanoparticle type as a function of pH shows preferential interactions between prisms at higher pH values (fewer protonated carboxylates) than spheres. (c) Observation of the SPR peak intensity for each particle type demonstrates reversibility in the association/dissociation process with pH after several cycles. (d) SAXS patterns for nanoparticle solutions at different pH values, confirming the selective formation of prism aggregates (arrow-labeled peak) over those composed of spheres.

prisms. In addition, with a high local effective concentration of DNA sticky ends and conformationally favorable duplexes, the rate of prism−prism dehybridization is further hindered. Thus, several mechanisms contribute to a reduced $k_{diss.}$ and thereby drive the enhancement to the overall rate of nanoprism association, allowing the system to arrive at a fully hybridized state more quickly.

Although DNA is an attractive ligand for investigating these shape-mediated effects, we also have probed the role of nanoparticle anisotropy in interparticle association with a carboxylic acid-terminated ligand to confirm the generality of these results (see Supporting Information for experimental details). Once anchored to the nanoparticles via a thiol linkage, these molecules present charged carboxylates at high pH, conferring colloidal stability (Figure 5a).[25,26] Upon protonation of the carboxylates by modification of the solution pH, hydrogen-bonding between neighboring carboxylic acid groups allows for interparticle association, consistent with previous reports.[25−28] As in the case of DNA, interparticle association between prisms occurs selectively compared to spheres, as fewer protonated carboxylates are required to facilitate prism−prism interactions because of the increased contact area and elevated local concentration of terminal functional groups induced by the particle shape (Figure 5b). Importantly, this interaction was found to occur at pH values consistent with the pK_a of the ligand[29,30] and was completely reversible with pH for several cycles (Figure 5c). Finally, SAXS was used to characterize the nanoparticle solutions at each stage of the reaction: all particles dispersed (pH 8.02), only prisms associated (pH 3.14), and both prisms and spheres associated (pH 2.00) (Figure 5d). Consistent with the previous results, nanoprisms associate in a face-to-face manner at higher pH values than spheres. Interestingly, these data also allow calculation of the median film thickness of each ligand shell, which reveals a larger value for prism aggregates (2.49 nm) than for sphere aggregates (1.33 nm). Detailed structural investigations on self-assembled monolayers of nearly identical ligands by Whitesides and co-workers have found film thickness values that more closely match those of the associated prisms (2.5−4.0 nm),[31,32] and may indicate that, as in the case of oligonucleotides, the ligand conformation on prisms is more favorable than that on spheres.

CONCLUSIONS

A combination of factors (an increased number of interparticle connections, an elevated local concentration of terminal DNA nucleotides, and an increased stability of DNA duplexes) contribute to the observed thermodynamic and kinetic enhancements to hybridization. Strikingly similar effects observed for a carboxylic acid-terminated oligo(ethylene glycol) ligand system are likely governed by the same mechanisms and suggest these findings may apply to a broad range of molecules. Indeed, we believe these results represent a new kind of shape-dependent nanoscale property wherein the collective behavior of nanoparticle ligands can vary significantly based on the shape of the nanoparticle on which they reside. Importantly, these results likely apply only to cases where ligands are under strong spatial confinement, have a terminal functional group mediating chemical interactions, and are rigid enough to preserve the shape of the scaffold to which they are anchored. However, these conditions are extremely common in nanoparticle systems and accurately describe the vast majority of ligand shells. Consequently, these results have implications in the field of anisotropic nanoparticle assembly and are likely relevant to a variety of research projects that seek to understand and govern the self-organization of nanostructures into new and complex architectures.[33−36]

ASSOCIATED CONTENT

Supporting Information. Full experimental details, description of thermodynamic and kinetic analyses, and additional figures. This material is available free of charge via the Internet at http://pubs.acs.org.

AUTHOR INFORMATION

Corresponding Author
chadnano@northwestern.edu

ACKNOWLEDGMENT

C.A.M. acknowledges the DOE for support of this work through the Non-equilibrium Energy Research Center, and the AFOSR and DDR&E for support through a MURI Award. M.R.J. is grateful to the NSF for a Graduate Research Fellowship and to Northwestern University for a Ryan Fellowship. R.J.M., A.E.P., and P.C.P. are grateful to Northwestern University for Ryan Fellowships. Portions of this work were carried out at the DuPont-Northwestern-Dow Collaborative Access Team (DND-CAT) beamline located at Sector 5 of the Advanced Photon Source (APS). DND-CAT is supported by E.I. DuPont de Nemours & Co., The Dow Chemical Co., and the State of Illinois. Use of the APS was supported by the U.S. Department of Energy, Office of Science, Office of Basic Energy Sciences, under Contract No. DE-AC02-06CH11357. This work made use of the J.B Cohen X-ray Diffraction Facility, supported by the MRSEC program of the National Science Foundation (DMR-1121262) at the Materials Research Center at Northwestern University.

REFERENCES

(1) Xia, Y.; Xiong, Y.; Lim, B.; Skrabalak, S. *Angew. Chem., Int. Ed.* **2009**, *48*, 60.
(2) Jones, M. R.; Osberg, K. D.; Macfarlane, R. J.; Langille, M. R.; Mirkin, C. A. *Chem. Rev.* **2011**, *111*, 3736.
(3) Jin, R. C.; Cao, Y. C.; Hao, E. C.; Metraux, G. S.; Schatz, G. C.; Mirkin, C. A. *Nature* **2003**, *425*, 487.
(4) Nikoobakht, B.; El-Sayed, M. A. *Chem. Mater.* **2003**, *15*, 1957.
(5) Kelly, K. L.; Coronado, E.; Zhao, L. L.; Schatz, G. C. *J. Phys. Chem. B* **2003**, *107*, 668.
(6) Bratlie, K. M.; Lee, H.; Komvopoulos, K.; Yang, P.; Somorjai, G. A. *Nano Lett.* **2007**, *7*, 3097.
(7) Glotzer, S. C.; Solomon, M. J. *Nat. Mater.* **2007**, *6*, 557.
(8) Jones, M. R.; Macfarlane, R. J.; Lee, B.; Zhang, J.; Young, K. L.; Senesi, A. J.; Mirkin, C. A. *Nat. Mater.* **2010**, *9*, 913.
(9) Mirkin, C. A.; Letsinger, R. L.; Mucic, R. C.; Storhoff, J. J. *Nature* **1996**, *382*, 607.
(10) Lytton-Jean, A. K. R.; Mirkin, C. A. *J. Am. Chem. Soc.* **2005**, *127*, 12754.
(11) Rosi, N. L.; Giljohann, D. A.; Thaxton, C. S.; Lytton-Jean, A. K. R.; Han, M. S.; Mirkin, C. A. *Science* **2006**, *312*, 1027.
(12) Alivisatos, A. P.; Johnsson, K. P.; Peng, X.; Wilson, T. E.; Loweth, C. J.; Bruchez, M. P.; Schultz, P. G. *Nature* **1996**, *382*, 609.
(13) Park, S. Y.; Stroud, D. *Phys. Rev. B* **2003**, *67*, 212202.
(14) Kiang, C.-H. *Physica A* **2003**, *321*, 164.
(15) Macfarlane, R. J.; Jones, M. R.; Senesi, A. J.; Young, K. L.; Lee, B.; Wu, J.; Mirkin, C. A. *Angew. Chem., Int. Ed.* **2010**, *49*, 4589.
(16) Hurst, S. J.; Hill, H. D.; Mirkin, C. A. *J. Am. Chem. Soc.* **2008**, *130*, 12192.
(17) Hill, H. D.; Hurst, S. J.; Mirkin, C. A. *Nano Lett.* **2008**, *9*, 317.
(18) Millstone, J. E.; Park, S.; Shuford, K. L.; Qin, L.; Schatz, G. C.; Mirkin, C. A. *J. Am. Chem. Soc.* **2005**, *127*, 5312.
(19) Millstone, J. E.; Wei, W.; Jones, M. R.; Yoo, H.; Mirkin, C. A. *Nano Lett.* **2008**, *8*, 2526.
(20) Millstone, J. E.; Georganopoulou, D. G.; Xu, X.; Wei, W.; Li, S.; Mirkin, C. A. *Small* **2008**, *4*, 2176.
(21) Ghosh, S. K.; Pal, T. *Chem. Rev.* **2007**, *107*, 4797.
(22) Marky, L. A.; Breslauer, K. J. *Biopolymers* **1987**, *26*, 1601.
(23) Bloomfield, V. A.; Crothers, D. M.; Tinoco, I. *Nucleic Acids Structures, Properties, and Functions*; University Science Books: Sausalito, CA, 2000.
(24) Macfarlane, R. J.; Lee, B.; Hill, H. D.; Senesi, A. J.; Seifert, S.; Mirkin, C. A. *Proc. Natl. Acad. Sci. U.S.A.* **2009**, *106*, 10493.
(25) Si, S.; Mandal, T. K. *Langmuir* **2006**, *23*, 190.
(26) Preston, T. C.; Nuruzzaman, M.; Jones, N. D.; Mittler, S. *J. Phys. Chem. C* **2009**, *113*, 14236.
(27) Han, L.; Luo, J.; Kariuki, N. N.; Maye, M. M.; Jones, V. W.; Zhong, C. J. *Chem. Mater.* **2002**, *15*, 29.
(28) Wang, L.; Luo, J.; Schadt, M. J.; Zhong, C.-J. *Langmuir* **2009**, *26*, 618.
(29) *CRC Handbook of Chemistry and Physics*, 77th ed.; CRC Press: Boca Raton, FL, 1996.
(30) Dippy, J. F. J.; Hughes, S. R. C.; Rozanski, A. *J. Chem. Soc.* **1959**, 2492.
(31) Harder, P.; Grunze, M.; Dahint, R.; Whitesides, G. M.; Laibinis, P. E. *J. Phys. Chem. B* **1998**, *102*, 426.
(32) Lahiri, J.; Isaacs, L.; Tien, J.; Whitesides, G. M. *Anal. Chem.* **1999**, *71*, 777.
(33) Morrow, T. J.; Li, M.; Kim, J.; Mayer, T. S.; Keating, C. D. *Science* **2009**, *323*, 352.
(34) Srivastava, S.; Santos, A.; Critchley, K.; Kim, K.-S.; Podsiadlo, P.; Sun, K.; Lee, J.; Xu, C.; Lilly, G. D.; Glotzer, S. C.; Kotov, N. A. *Science* **2010**, *327*, 1355.
(35) Chen, C.-L.; Zhang, P.; Rosi, N. L. *J. Am. Chem. Soc.* **2008**, *130*, 13555.
(36) Macfarlane, R. J.; Lee, B.; Jones, M. R.; Harris, N.; Schatz, G. C.; Mirkin, C. A. *Science* **2011**, *334*, 204.